

NUMERICAL MODELING OF NUCLIDE TRANSPORT IN STRUCTURES AND THE NEAR FIELD OF A NEAR-SURFACE RADIOACTIVE WASTE DISPOSAL FACILITY

Anisimov N. A., Kuvaev A. A., Sizonenko E. V.

FSBI “Hydrospetzgeologiya”, Moscow, Russia

Article received on September 29, 2023

The paper considers a numerical model of radionuclide transport in the structural elements of a near-surface radioactive waste disposal facility (NSDF). It presents a calculation of a nuclide flow from the NSDF into the underlying rocks and groundwater considering three characteristic groups of radionuclides: long-lived weakly absorbable, long-lived absorbable and relatively short-lived (with a half-life of up to 31 years). The study demonstrates how the sorption properties of the engineered barriers, their geometric characteristics, as well as the features of radioactive waste package layout may influence radionuclide releases from the waste disposal facility into groundwater.

Keywords: NSDF structures, safety barriers, RW packages, distribution coefficient, release rate at the groundwater table, variation of parameter values, flow permeability, radioactive waste.

Introduction

The article is a continuation of a study [1] exploring a numerical model of moisture seepage through NSDF structures, which, along with diffusion, is seen as the main physical process driving radionuclide transport in structural materials of radioactive waste (RW) disposal facilities and their release beyond their boundaries.

The study [1] shows how gradual degradation of concrete NSDF elements occurring over a period of up to 1,000 years after its closure affects the spatial pattern of seepage flows formed in the NSDF structures. This study mainly emphasizes on the long-term forecasts regarding radionuclide releases outside the NSDF structures over extended periods of tens and hundreds of thousands of years contingent on the potential hazard of the RW disposed of there [2].

A system of safety barriers (SBS) is used to prevent and reduce potential radioactive releases beyond the NSDF structures. On the one hand, it reduces the amount of water seeping into RW disposal compartments, and on the other hand, it retards radionuclide transport due to its sorption properties.

SBS performance depends on a combination of its geometric characteristics and sorption-capacitive properties. In this regard, it is of interest to study the characteristics of SBS elements and the way they influence the transport of radionuclides contained in the RW and their release beyond the NSDF boundaries, which was exactly the task of this study that have been addressed based on computational modeling using the COMSOL Multiphysics software package [3].

NSDF design layout and the geometry of the calculation model

Figure 1 presents the geometry of a calculation model built based on a prototype NSDF design layout [1], [4].

The model involves the following engineered safety barriers (EB):

- EB1 – walls and waste form material of the RW packages;
- EB2 – buffer material (clay powder) filling the gaps between the compartment walls and the RW packages;
- EB3 – concrete walls – 800 mm, bottom slab – 1,000 mm, top slab – 250 mm;
- EB4 – clay retainer around the NSDF perimeter (walls, bottom slab) - 1,000 mm;
- EB5 – overlying multi-layer structure (from top to bottom):
 - soil-vegetation layer – 200 mm;
 - drainage layer – 420 mm;
 - bentomat (1st layer) – 30 mm;
 - compacted clay or loam – 1,170 mm;
 - sand – 200 mm;
 - bentomat (2nd layer) – 30 mm.

In addition, there's a natural safety barrier represented by the host rocks.

The calculation model assumes that waste referred to RW Class 4 is disposed of in metal containers in the three upper tiers and RW Class 3 – in reinforced concrete containers in the bottom one. Their dimensions were set according to those of the KMZ and NZK-150-1.5P containers [5].

The model (Figure 1) also defines a host rock area of 80×30 m and indicates the groundwater level (GWL). Its characteristics were set based on survey findings describing an actual facility [4]: water-bearing sediments were represented by loams, the GWL depth relevant to the ground surface level accounted for 12 m.

Calculation model

Radionuclide transport in the saturated-unsaturated zone was calculated based on a mass transfer equation describing a non-stationary concentration field for radioactive substances [6]:

$$(n + K_d \rho_n) \frac{\partial C}{\partial t} + \nabla(\bar{v}C) - \nabla(nD\nabla C) + \lambda(n + K_d \rho_n)C = 0 \quad (1)$$

where n is the moisture content; K_d —sorption distribution coefficient in the water—host rock system (m^3/kg); ρ_n is the density of dry water-containing material (kg/m^3); C is the specific activity of the radionuclide in a liquid phase (kg/m^3); \bar{v} is the flow velocity vector (m/day); D is the tensor of the total dispersion coefficient (m^2/day); λ is the radioactive decay constant ($1/day$).

The total dispersion coefficient includes components describing molecular diffusion and hydrodynamic dispersion processes. According to [7], [8], in a general case, the total dispersion coefficient D is a tensor of a second rank. For a porous medium it can be represented as follows:

$$nD_{ij} = D_{ij}^d + D_m \delta_{ij} = D_{ij}^d + \chi n D_m^0 \delta_{ij}$$

$$D_{ij}^d = (\delta_L - \delta_T) \frac{v_i v_j}{|\bar{v}|} + \delta_T |\bar{v}| \delta_{ij}$$

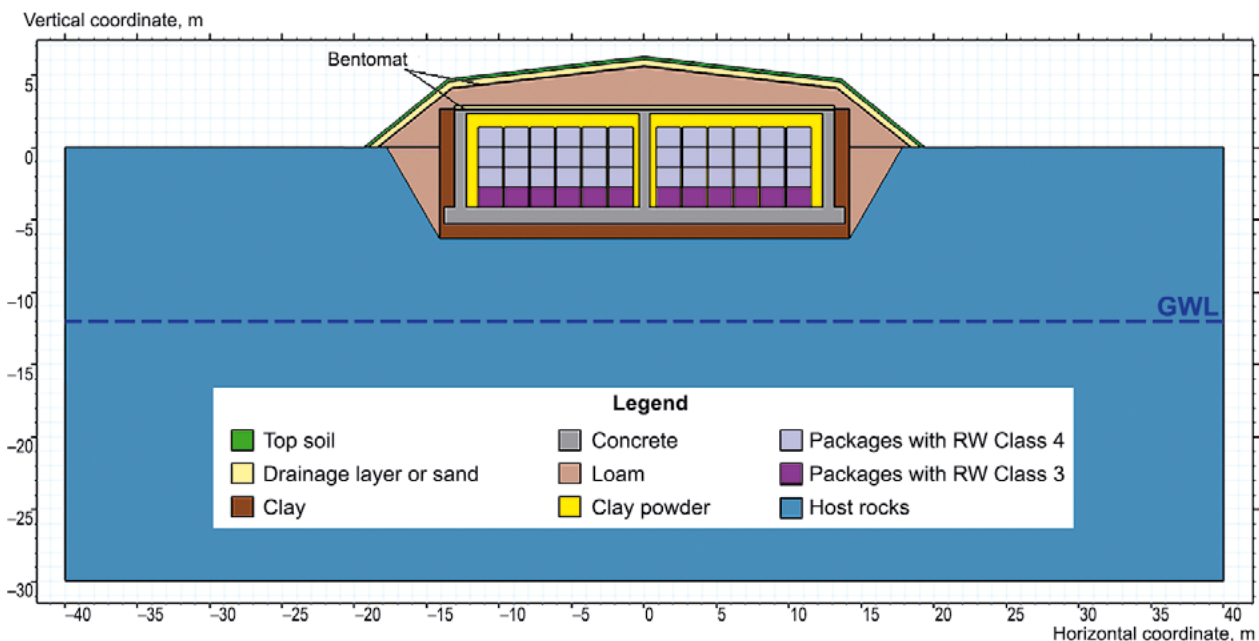


Figure 1. Geometry of the calculation model

where D_{ij}^d is a coefficient describing hydrodynamic dispersion (m^2/day); D_m stands for the effective molecular diffusion coefficient (m^2/day); χ is the tortuosity of seepage channels in a porous medium; D_m^0 is the molecular diffusion coefficient in a free medium; δ_L and δ_T are the parameters of longitudinal and transverse dispersion respectively (m); $|\bar{v}|$ is a module of the seepage transfer velocity vector (m/day); v_i and v_j represent the projections of the seepage transfer velocity vector \bar{v} onto the corresponding coordinate axes (m/day); δ_{ij} is the Kronecker delta function that can be calculated as follows:

$$\delta_{ij} = \begin{cases} 1 & \text{if } i = j \\ 0 & \text{if } i \neq j \end{cases} \quad i, j = 1, 2, 3$$

Since the NSDF structures prevail considerably in their longitudinal dimension over the transverse one [4], computational modeling is performed in a two-dimensional (cross-sectional) layout.

Parameters n (moisture content) and \bar{v} (seepage transfer velocity vector) included in (1) were calculated based on a seepage transfer model and the Richards equation, the formulation of which for the considered NSDF design layout was given in [1].

The calculations have addressed the following radionuclides: 3H , ^{14}C , ^{36}Cl , ^{90}Sr , ^{99}Tc , ^{129}I , ^{137}Cs , ^{226}Ra , ^{232}Th , ^{238}U , ^{237}Np , ^{239}Pu , ^{241}Am , ^{245}Cm .

The initial specific activity levels for the radionuclides found in the RW packages were set according to those presented in Table 1. These values corresponded to the activity levels of radionuclides in the RW Class 3 and 4 disposed of in NSDF [9].

Table 1. Initial specific activity levels for radionuclides in RW packages, Bq/m³

| RW class | β -emitters $^3H, ^{14}C, ^{36}Cl, ^{90}Sr, ^{99}Tc, ^{129}I, ^{137}Cs$ | α -emitters $^{226}Ra, ^{232}Th, ^{238}U$ | Transuranium α -emitters $^{237}Np, ^{239}Pu, ^{241}Am, ^{245}Cm$ |
|----------|--|---|---|
| Class 3 | $6 \cdot 10^{13}$ | $9 \cdot 10^8$ | $2 \cdot 10^8$ |
| Class 4 | $2 \cdot 10^{10}$ | $3 \cdot 10^7$ | $6 \cdot 10^6$ |

Table 2 shows the half-lives of radionuclides used in the calculations and the distribution coefficients calculated based on averaged data from literature sources [10]–[12].

Long-term degradation of concrete expected mainly in the first thousand years after NSDF closure [13] have not been considered in this study since it was basically focused on providing long-term forecasts. The calculations assumed that concrete structures and RW packages have degraded, only the buffer material backfilling the internal space in the repository compartments, the clay retainer installed in the bottom part and along the NSDF perimeter, as well as the materials of the overlying cover, with the exception

of the bentomat that was considered damaged, were assumed as the barriers that managed to retain their performance. The distribution coefficients for the material of the degraded concrete and RW packages were assumed as being equal to those of sand (Table 2).

Table 2. Half-lives and distribution coefficients of radionuclides adopted for the construction NSDF materials and water-bearing sediments in the near field

| Radio-nuclide | Half-life, years | Distribution coefficient, m ³ /kg | | | |
|---------------|----------------------|--|---------|------------------------|-------------|
| | | sand | loam | clay (external screen) | clay powder |
| 3H | 12.3 | 0.0001 | 0.02 | 0.03 | 0.03 |
| ^{14}C | $5.73 \cdot 10^3$ | 0.001 | 0.001 | 0.001 | 0.001 |
| ^{36}Cl | $3.01 \cdot 10^5$ | 0.0008 | 0.00025 | 0.0004 | 0.0004 |
| ^{90}Sr | 29.1 | 0.004 | 0.0065 | 0.11 | 0.1 |
| ^{99}Tc | $2.13 \cdot 10^5$ | 0.0001 | 0.0001 | 0.001 | 0.001 |
| ^{129}I | $1.57 \cdot 10^7$ | 0.001 | 0.001 | 0.001 | 0.001 |
| ^{137}Cs | 30.1 | 0.28 | 4.6 | 1.9 | 0.2 |
| ^{226}Ra | $1.60 \cdot 10^3$ | 0.5 | 9 | 9 | 0.1 |
| ^{232}Th | $1.40 \cdot 10^{10}$ | 3 | 5.8 | 5.8 | 0.3 |
| ^{238}U | $4.47 \cdot 10^9$ | 0.035 | 0.025 | 0.15 | 0.1 |
| ^{237}Np | $2.14 \cdot 10^6$ | 0.005 | 0.025 | 0.055 | 0.1 |
| ^{239}Pu | $2.41 \cdot 10^4$ | 0.34 | 1.2 | 5.1 | 0.3 |
| ^{241}Am | 432 | 0.34 | 9.6 | 8.4 | 0.3 |
| ^{245}Cm | $8.50 \cdot 10^3$ | 4 | 6 | 6 | 4 |

For all nuclides and materials, averaged D_m (molecular diffusion coefficient), δ_L and δ_T (longitudinal and transverse dispersion parameters) were set, i. e., $2 \cdot 10^{-10} m^2/s$, 0.1 m and 0.01 m respectively ([8], [14]).

The studied radionuclides were conventionally divided into three groups: short-lived, weakly absorbable long-lived, well absorbable long-lived radionuclides. Table 3 presents their breakdown according to these groups.

Table 3. Radionuclide break down into groups

| Groups of radionuclides | General characteristics | Radionuclides |
|-------------------------|------------------------------|---|
| Group 1 | Short-lived* | $^3H, ^{90}Sr, ^{137}Cs$ |
| Group 2 | Weakly absorbable long-lived | $^{14}C, ^{36}Cl, ^{99}Tc, ^{129}I$ |
| Group 3 | Well absorbable long-lived | $^{226}Ra, ^{232}Th, ^{238}U, ^{237}Np, ^{239}Pu, ^{241}Am, ^{245}Cm$ |

* conditionally short-lived with a half-life of less than 31 years

Further, the study considers some specific features describing the release of these three groups of radionuclides from the NSDF and their release to the GWL.

Models for the Safety Analysis of Radioactive Waste Disposal Facilities

Calculations were performed using the finite element method implemented in the COMSOL Multiphysics software package [3]. As in [1], the model involved an irregular triangular mesh with a total of ~160,000 computational cells.

Modeling results: specific features of radionuclide transport in the structural NSDF elements

Radionuclide release from a NSDF basically occurs in three stages:

- initial state and distribution within the structural repository boundaries;
- transport in the aeration zone — areas above the GWL;
- radionuclides reach the GWL and spread with groundwater.

As an example, Figure 2 shows the specific activity fields for ^{238}U considering three points in time characterizing the above stages.

One can see that uranium release outside the repository structure mainly occurs in two relatively narrow areas indicated by red arrows, which is explained by some specific nature of seepage flow formation inside the repository structure after the degradation of its concrete walls and bottom slabs starts.

Figure 3 shows the seepage flows pictured as a vector velocity field.

Since degraded concrete structures are characterized by relatively high seepage coefficients compared to other NSDF construction materials, the seepage

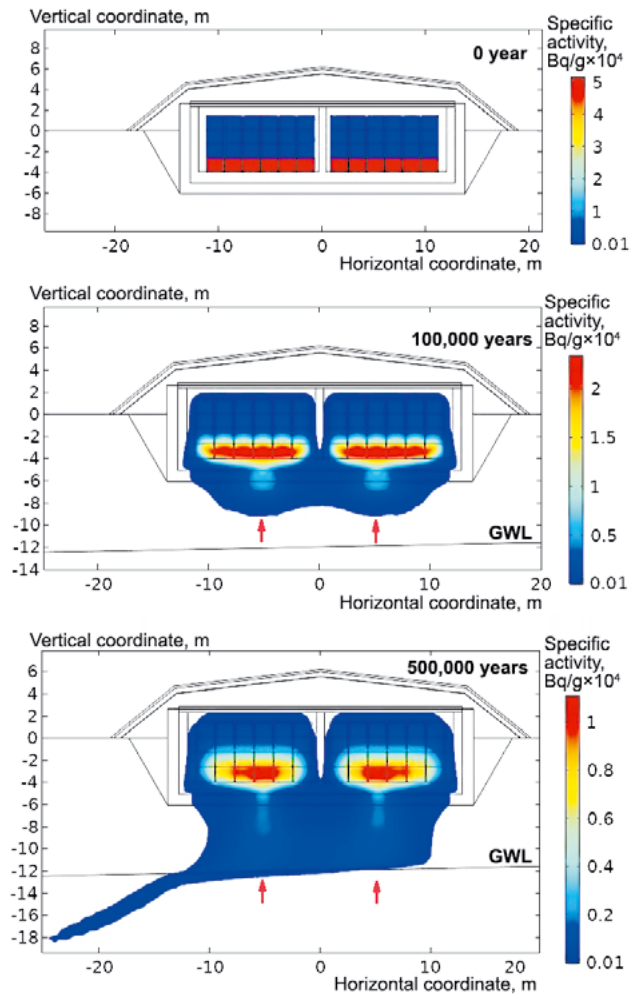


Figure 2. Specific activity of ^{238}U in the pore water of NSDF structures and near field rocks (red arrows show the areas of predominant radionuclide releases)

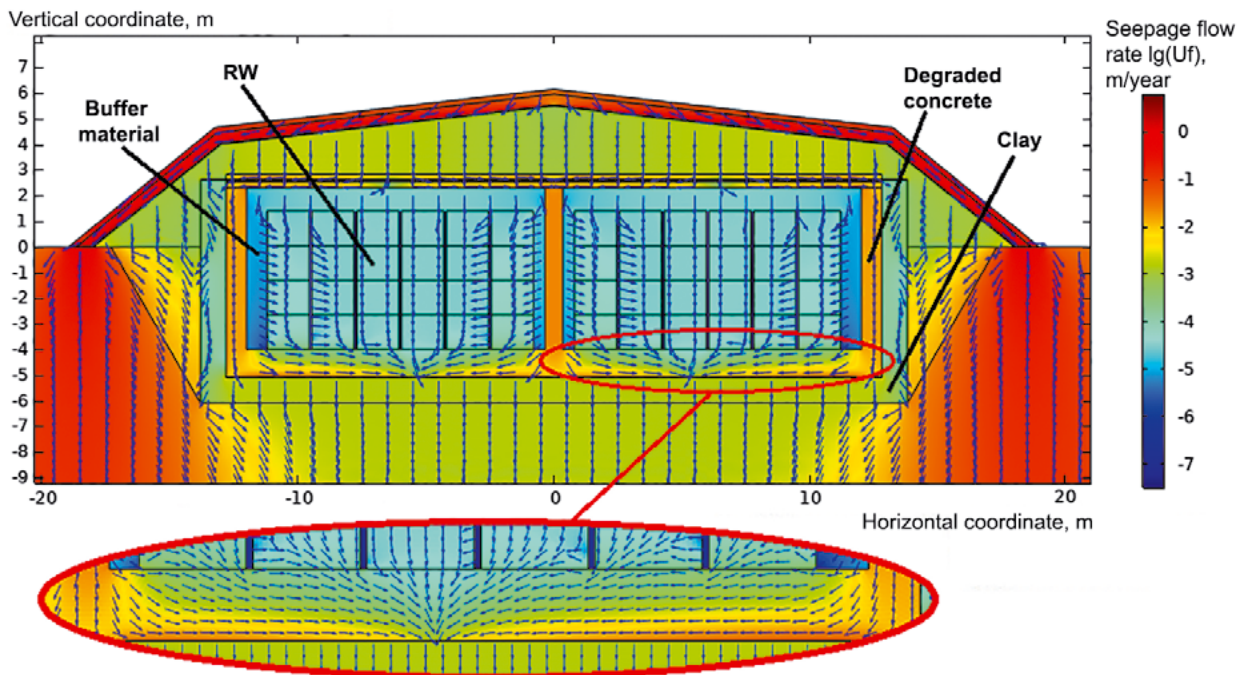


Figure 3. Flow rate field for water seeping through the structural NSDF elements and the near field rocks and counter seepage flows formed in the degraded concrete layer

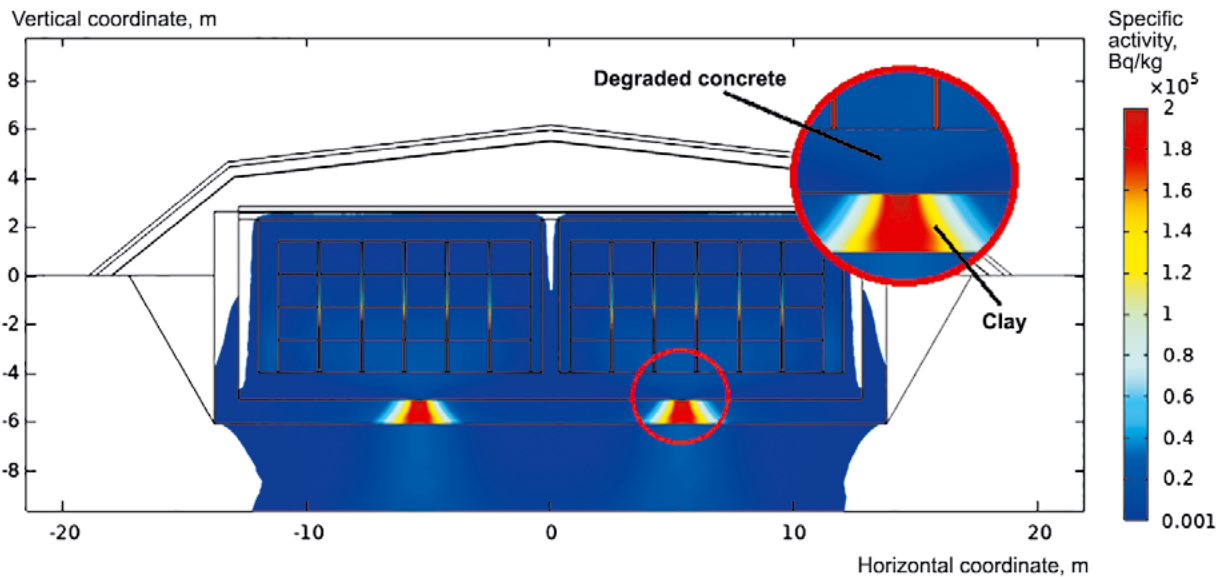


Figure 4. Distribution of ^{238}U specific activity in the structural NSDF elements and the host rocks (calculated over a period of 500,000 years)

flows would be mainly concentrated exactly there. Thus, water would predominantly flow along the vertical and horizontal elements of the degraded concrete.

Counter water flows are formed above the bottom clay layer, which dwindle as they approach each other. Radionuclides leached from the RW packages move to the upper part of these flows discharged into a clay layer in a narrow area where the flows converge. Thus, radionuclide transport and sorption in the clay layer is spatially limited and only a small fraction of the clay volume would act as a sorption barrier. This is reflected in Figure 4 showing the distribution of specific activities for ^{238}U sorbed by the structural repository elements and the host rocks.

Modeling results: radionuclide release to the GWL

Under the long-term safety assessments (LSA), a calculation model representing a NSDF is usually coupled with a regional geological flow and transport model to identify the spread of nuclides along with groundwater flows. These two models are coupled according to the GWL. Thus, when radionuclide transport from a NSDF is modeled, it mainly shows their flows released to the GWL, which is used as an output source function in the regional model.

Modeling results showed that provided the considered design of the repository structures and the host rock characteristics, Group 1 radionuclides would not be released to the GWL in quantities able to affect the LSA results. They are expected to decay to values below the intervention level (IL) [15] remaining either within the repository boundaries or getting released into the aeration zone, but not reaching the GWL in considerable concentrations.

Figures 5, 6 show the intensity of Group 2 and 3 radionuclides releases to the GWL.

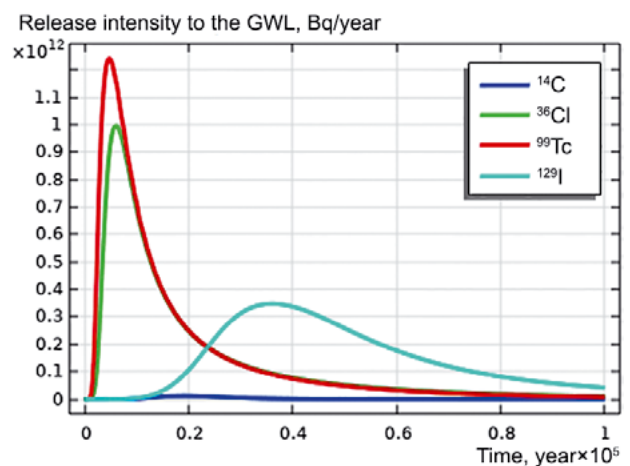


Figure 5. Intensity of Group 2 radionuclide releases to the GWL

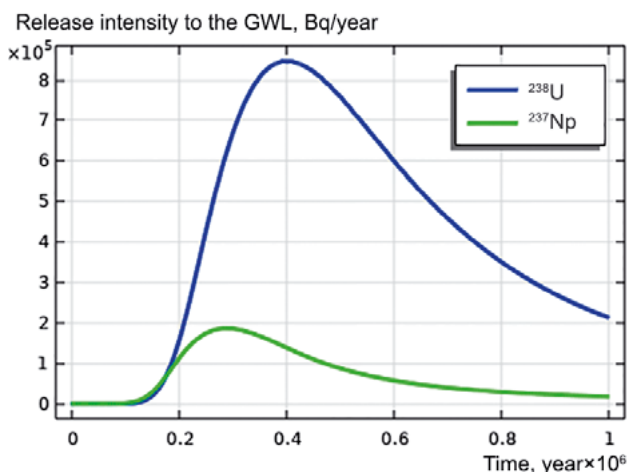


Figure 6. Intensity of ^{238}U u ^{237}Np releases to the GWL

All radionuclides referred to Group 2 and two of those referred to Group 3, namely, ^{238}U and ^{237}Np release to the GWL. Isotopes of Group 3, namely, ^{226}Ra , ^{232}Th , ^{239}Pu , ^{241}Am , ^{245}Cm are well sorbed by the repository safety barrier materials and the host rocks (Table 2) and do not reach the GWL in considerable concentrations.

Thus, the repository designs are expected to protect the groundwater from the spread of short-lived (with a half-life of less than 31 years) and some long-lived well absorbable radionuclides even given the degraded concrete elements, but the buffer material, the clay retainer and the host rocks that nevertheless preserve their integrity and properties.

Modeling results: variation in the EB properties and changes in the RW package layout

Parameters of calculation models applied under long-term safety assessments are to a greater or lesser degree characterized by some uncertainty that can be associated both with the insufficiency or inaccuracy of the initial data and the natural variability of the measured properties [16] and changes in the material properties driven by various factors at the post-closure stage.

Possible variations in parameter values were considered based on a case study of ^{238}U release from a NSDF.

Figure 7 shows the calculated intensity of its release to the GWL provided some changes in the Kd_{EB4} , which is the distribution coefficient for the clay retainer material. These values have been assigned by the kKd multiplier by applying it to the initial clay distribution coefficient of $0.15 \text{ m}^3/\text{kg}$. Other parameters of the calculation model remained unchanged.

At $kKd=0.01-0.2$, the graphs presented in Figure 7 are almost identical, whereas at $kKd=5$ they follow the abscissa axis.

To further analyze the obtained results, the W_{\max} characteristic was introduced representing the dependence between the maximum intensity of nuclide release to the GWL shown in the graphs and a variable parameter. In case of graphs shown in Figure 7, the variable parameter was assumed as Kd_{EB4} . Figure 8 shows the dependence between the W_{\max} and Kd_{EB4} calculated from these graphs.

Three areas can be distinguished in the graph shown in Figure 8:

- 1— area impermeable to radionuclide transport in the barrier — at $Kd_{EB4} > 0.76 \text{ m}^3/\text{kg}$;
- 2— transition area — $Kd_{EB4} = 0.03-0.76 \text{ m}^3/\text{kg}$;
- 3— area transparent to radionuclide transport in the barrier — at $Kd_{EB4} < 0.03 \text{ m}^3/\text{kg}$.

The shape of this graph demonstrates that when the values of the distribution coefficient remain in

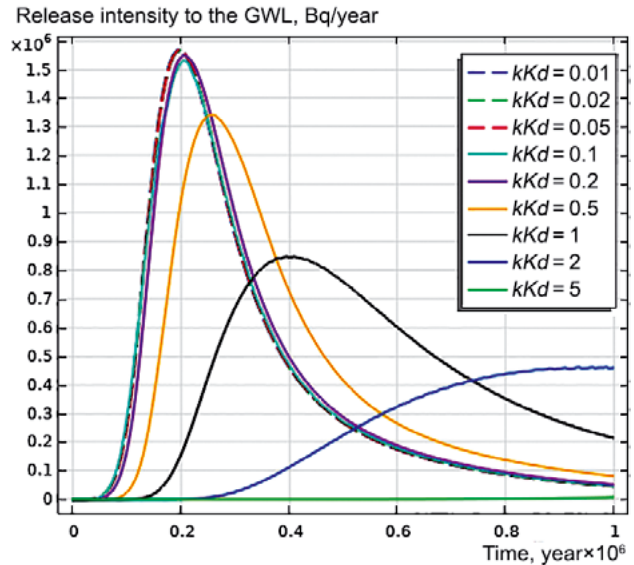


Figure 7. Intensity of ^{238}U release to the GWL calculated assuming the $Kd_{EB4} = kKd \times 0.15 \text{ m}^3/\text{kg}$

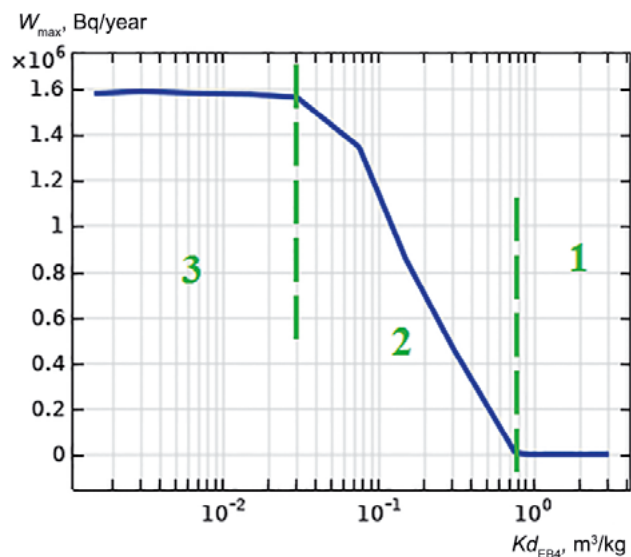


Figure 8. Dependence between the maximum intensities of ^{238}U release to the GWL and the Kd_{EB4}

area 1, no nuclides would get released to the GWL within a given time period (1 million years), and on the other hand, given any Kd values being below the threshold level ($\sim 0.03 \text{ m}^3/\text{kg}$), the intensity of nuclide release to the GWL would remain constant in area 3.

The graph shown in Figure 8 conventionally called the Threshold Flow Curve (TFC) is not an isolated characteristic of a single safety barrier as it depends on other barriers and the totality of their properties imposing their own restrictions on nuclide flow rates. This explains the constant nature of W_{\max} at $Kd_{EB4} < 0.03 \text{ m}^3/\text{kg}$.

In addition to the distribution coefficients specific for the safety barrier materials, their flow

permeability is affected by their geometric characteristics. Figure 9 shows the W_{\max} calculated assuming various thickness of the clay retainer in the foundation of the NSDF structure designated as Y_{EB4} (Kd_{EB4} remains constant and equal to the initial value of $0.15 \text{ m}^3/\text{kg}$).

In the main part of the graph shown in Figure 9, an increase in the EB4 thickness results in a lower intensity of radionuclide release to the GWL. However, this pattern is violated when the barrier thickness is less than 0.25 m, starting from which a decrease in Y_{EB4} would cause a sudden drop in W_{\max} . Thus, according to its performance, clay barrier thickness of $\sim 3 \text{ m}$ would become equivalent to its complete absence.

This result can be explained by the fact that a decrease in the clay layer thickness from 0.3 m would change the seepage flow pattern in the degraded concrete layer overlying the RW packages, which is reflected in Figure 10. The flow in this layer would be more uniform and its rates in the bottom part of the RW disposal area would get lower resulting in

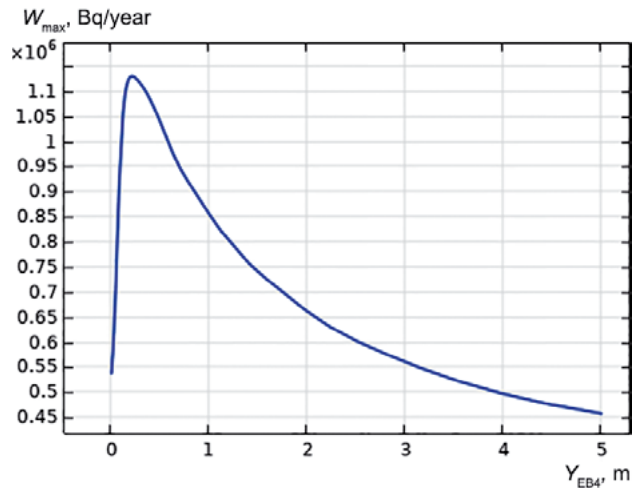


Figure 9. Dependence between the maximum intensity of ^{238}U release to the GWL (W_{\max}) and the clay retainer thickness (Y_{EB4})

a lower intensity of radionuclide leaching from the packages and, ultimately, a generally less intense radionuclide release into groundwater.

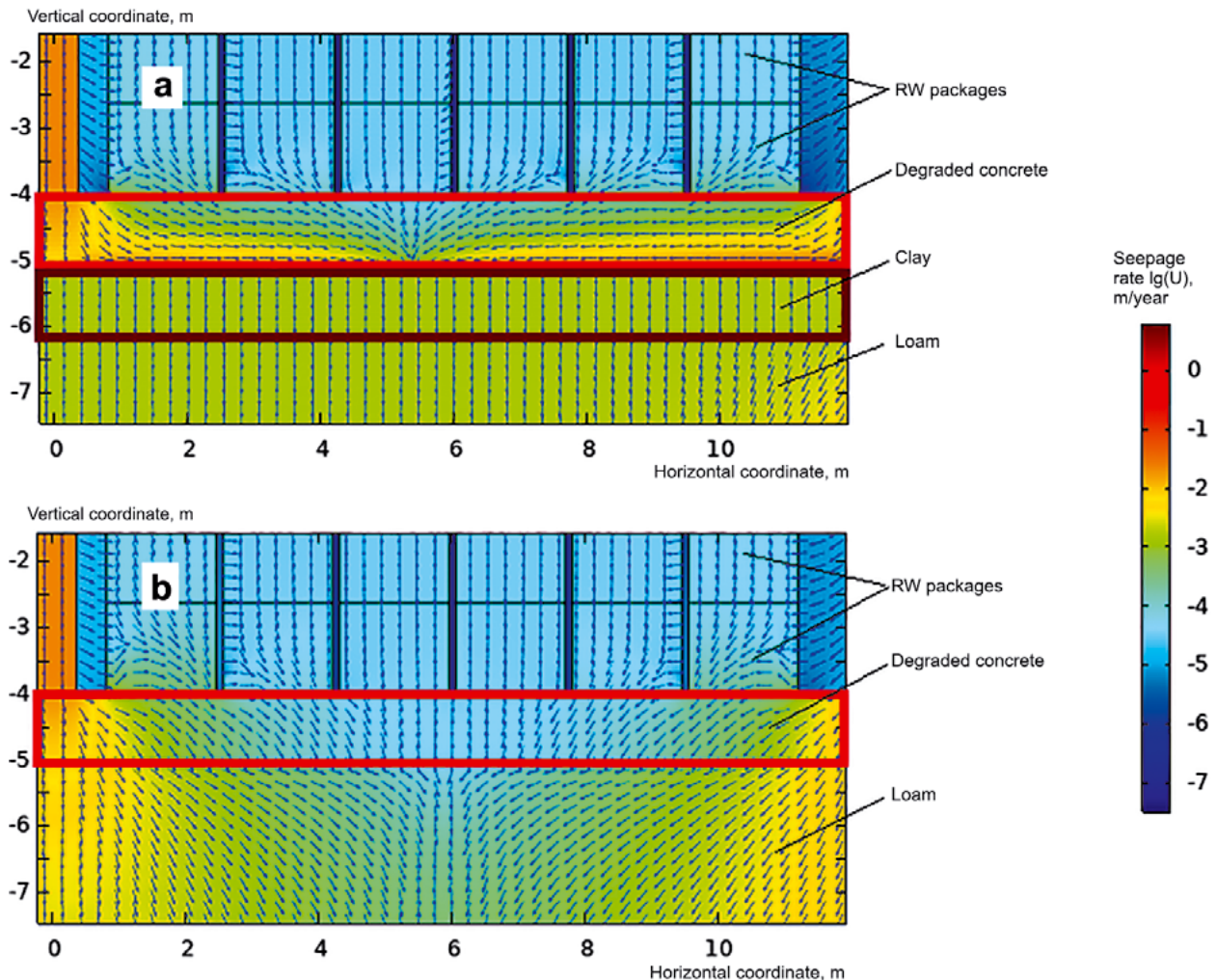


Figure 10. Field of water seepage rates in the bottom section of the NSDF structure (fragment):
a – in the presence of a 1-m-thick clay retainer; b – in the absence of a clay retainer

Another consequence related to the specific aspects of seepage flow formation in NSDF structures is that the intensity of radionuclide releases from them can be possibly reduced by changing the arrangement of the RW packages. Figure 11 shows graphs with calculated rates of ^{238}U release considering two options of RW package arrangement in the two bottom tiers:

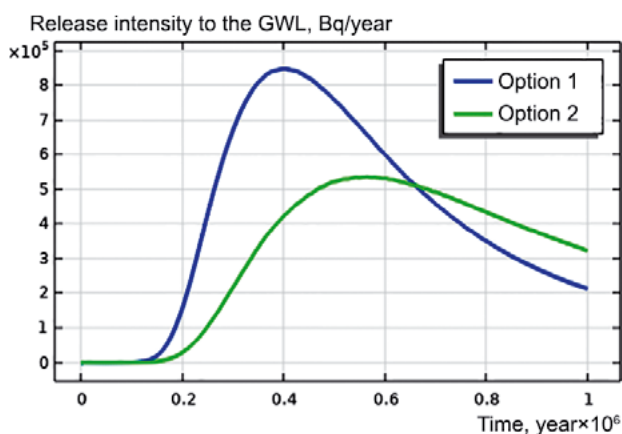


Figure 11. Intensity of ^{238}U release to GWL assuming two possible RW package layouts

- option 1 (basic): RW Class 3 packages are stacked in the bottom tier (as shown in Figure 1);
- option 2: RW Class 4 packages are stacked in the bottom tier overlaid by a single tier of RW Class 3 packages with two tiers of RW Class 4 packages above.

According to the given result, such rearrangement of RW package layouts would yield a 1.5-fold decrease in the maximum possible ^{238}U release from the NSDF. In general, this result shows that the safety of a NSDF can be possibly enhanced by optimizing the RW package layout.

Sensitivity of calculation results to variations in the parameters of the calculation model and its analysis

The above influence of parameter variations, i. e., clay distribution coefficients and clay layer thickness, on the calculation results was estimated separately provided the rest of the NSDF material characteristics assumed as constant. Thus, according to [16], this approach can be referred to local sensitivity assessment methods.

Several parameters can be compared simultaneously considering the degree of their influence on the ultimate result based on algorithms referred to the global sensitivity assessment methods. These methods were implemented in the COMSOL PC uncertainty assessment unit.

Figure 12 shows the estimated sensitivity of W_{\max} assumed as the target variable to variations in three parameters: the diffusion coefficient (D_m) and distribution coefficients for clay (Kd_{clay}) and buffer material (Kd_{buf}). Sensitivity was estimated based on the Morris method [17].

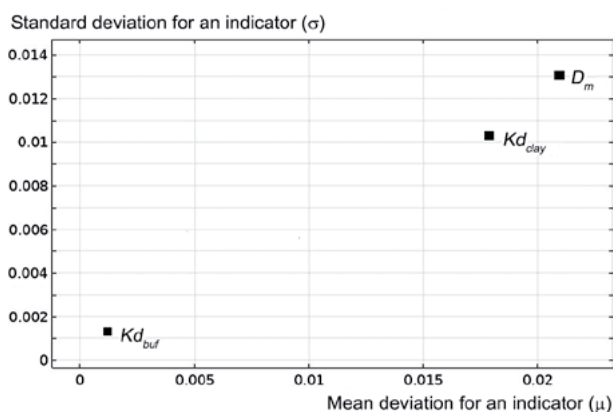


Figure 12. Scatter diagram for D_m , Kd_{clay} and Kd_{buf} indicators based on the Morris method

The results were presented considering two sensitivity indicators: mean value (μ) and standard deviation (σ). The former one is used to evaluate the overall impact of a varying parameter on the result and to compare it with the contribution produced by other parameters. The latter one (standard deviation) indicates whether there's a correlation between input data and gives an idea of how much influence a variation in one parameter has on the ultimate sensitivity assessment according to other parameters.

Figure 12 evidences that among the three parameters considered, the W_{\max} is most greatly affected by the diffusion coefficient and lastly by the distribution coefficient of the clay powder material. The latter result can be explained by the fact that, given its relatively thin interlayers, the predominant process contributing to RW transport in the RW disposal area would account for diffusion occurring over long-term intervals. In this case, the clay powder would mainly act not as a transport barrier, but a seepage barrier preventing moisture ingress into the RW seeping inside the repository structure.

Conclusion

A computational study of a prototype NSDF design yielded the following results:

1. Radionuclides that can be conditionally referred to the short-lived category (with a half-life of less than 31 years) and some long-lived radionuclides are retained within the NSDF structures and the aeration zone throughout the entire computational

modeling period of 1 million years causing no considerable releases to the groundwater.

2. The pronounced seepage flow heterogeneity in the NSDF structures, identified in the first part of this study [1], mainly explains the predominance of radionuclide transport flows in the narrow areas of the safety barriers reducing their performance in a quite considerable way.

3. Two threshold coefficients describing the distribution of radionuclides in the clay retainer material have been identified:

- $Kd_{EB4} > 0.76 \text{ m}^3/\text{kg}$ — the area impermeable for radionuclide transport in the barrier;
- $Kd_{EB4} < 0.03 \text{ m}^3/\text{kg}$ — the area transparent for radionuclide transport in the barrier.

In the former area, radionuclides do not reach the GWL during a given time period (1 million years), whereas in the latter one, the intensity of their release to the GWL depends in no way on the Kd variations.

4. The studied effects of variations in the clay retainer thickness on the ^{238}U release rate from NSDF showed that transport barrier in the form of a clay retainer was ineffective and this concept could be abandoned.

5. By changing the arrangement of RW Class 3 and 4 package layouts one may decrease the radionuclide release from the NSDF and, thus, enhance its safety.

6. The sensitivity assessment showed that in case of porous medium, variations in the radionuclide diffusion coefficient would greatly affect the calculation results. Thus, it should be identified experimentally with the highest possible accuracy and on an individual basis for the considered materials and isotopes.

The presented findings are valid for the considered NSDF design, RW composition, characteristics of the safety barrier materials and environmental conditions. The results may be similar provided some differences in the initial data, nevertheless the quantitative indicators would differ, which requires the computational modeling to be run considering each specific NSDF design option.

This paper studies only a small proportion of the parameters characterizing near-surface disposal facilities and the RW disposed of there. However, it also shows the fundamental need for two- and three-dimensional modeling since linear and chamber modeling methods, which are still used in the computational assessment of RW repositories, are not able to consider the spatial features of the evolving processes, thus, the resulting errors in the long-term safety assessment findings may amount to orders of magnitude [18], [19], [20].

References

1. Anisimov N. A., Kuvaev A. A. Chislennoe modelirovanie vlagoperenosa v konstruktsiyakh pripoverkhnostnogo punkta zakhroneniya radioaktivnykh otkhodov [Numerical Modeling of Moisture Transfer in the Structures of a Near-Surface Radioactive Waste Disposal Facility]. *Radioaktivnye otkhody — Radioactive Waste*, 2022, no. 3 (20), pp. 97–106. DOI: 10.25283/2587-9707-2022-3-97-106.
2. NP-055-14. *Zakhroneniye radioaktivnykh otkhodov. Printsipy, kriterii i osnovnyye trebovaniya bezopasnosti* [NP-055-14 Radioactive Waste Disposal. Principles, Criteria and Basic Safety Requirements].
3. Kovalenko A., Uzdanova A., Urtenov M., Nikonenko V. *Matematicheskoye modelirovaniye fiziko-khimi-cheskikh protsessov v srede Comsol Multiphysics 5.2*. [Mathematical modeling of physical and chemical processes in the Comsol Multiphysics 5.2 software]. Saint-Petersburg, Publishing House Lan' Publ., 2017. 228 p.
4. *Materialy obosnovaniya litsenzii na razmeshcheniye i sooruzheniye pripoverkhnostnogo punkta zakhroneniya tverdykh radioaktivnykh otkhodov 3 i 4 klassov, Tomskaya oblast', gorodskoy okrug ZATO Seversk* [Siting and Construction License Application for a Near-surface Disposal Facility for Solid Radioactive Waste Class 3 and 4, Tomsk region, urban district of the Restricted Access Territory Seversk]. Vol. 1. Moscow, FSUE NORAO Publ., 2018.
5. Sorokin V. T., Demin A. V., Kashcheyev V. V., Iroshnikov V. V., Gataullin R. M., Medelyayev I. A., Peregudov N. N., Sharafutdinov R. B. Konteynery dlya radioaktivnykh otkhodov nizkogo i srednego urovnya aktivnosti [Containers for Radioactive Waste Low and Medium Activity Level]. *Yadernaya i radiatsionnaya bezopasnost' — Nuclear and Radiation Safety*, 2013, no. 2 (68), pp. 15–22.
6. Shestakov V. M. *Gidrogeodinamika* [Hydrogeodynamics]. Moscow, Moscow University Publ., 1995. 368 p.
7. Fitts Ch. R. *Groundwater Science*. USA, San Diego, California, Academic Press, 2002.
8. Rumynin V. G. *Geomigratsionnyye modeli v gidrogeologii* [Geological transport modelling in hydrogeology]. Saint-Petersburg, Nauka Publ., 2011. 1160 p.
9. Decree of the Government of the Russian Federation No. 1069 of October 19, 2012.
10. Sharafutdinov R. B., Stroganov A. A., Levin A. G. et al. *Geologo-geokhimicheskiye aspekty zakhroneniya radioaktivnykh otkhodov* [Geological and geochemical aspects of radioactive waste disposal]. Nauchnyye i tekhnicheskiye aspekty okhrany okruzhayushchey sredy [Scientific and technical aspects of the environmental protection]. VINITI. 1999. Issue 5. Pp. 2–91.

11. Thibault D. H., Sheppard M. I., Smith P. A. *A Critical Compilation and Review of Default Soil Solid/Liquid Partition Coefficients, K_d , for Use in Environmental Assessments*. Atomic Energy of Canada Ltd., Whiteshell Nuclear Research Establishment, AECL-10125, Pinawa, Manitoba, Canada, 1990. 115 p.
12. B. Heuel-Fabianek. *Partition Coefficients (K_d) for the Modelling of Transport Processes of Radionuclides in Groundwater*. Technical Report Jül-4375, May 2014. DOI: 10.13140/2.1.4064.9608.
13. *Safety Assessment Methodologies for Near Surface Disposal Facilities* : Results of a Co-Ordinated Research Project. Vol. 1 and 2. IAEA, Vienna, 2004.
14. Fitts Ch. R. *Groundwater Science*. USA, California, San Diego, Academic Press, 2002. 450 p.
15. NRB-99/2009. *Sanitarnyye pravila i normativy* [Sanitary Rules and Regulations] SanPiN 2.6.1.2523-09. *Normy radiatsionnoy bezopasnosti* [Radiation Safety Standards]. Moscow, 2009.
16. Saveleva E. A., Svitelman V. S. Obrashchenie s neopredelennostyami v zadachakh raschetnogo obosnovaniya dolgovremennoi bezopasnosti [Uncertainty management in the context of long-term safety assessment]. *Radioaktivnye otkhody — Radioactive Waste*, 2022, no. 3 (20), pp. 61–71. DOI: 10.25283/2587-9707-2022-3-61-71.
17. Morris M. D. Factorial sampling plans for preliminary computational experiments. *Technometrics*, 1991, vol. 33, no. 2, pp. 161–174.
18. Anisimov N. A., Drozhko E. G., Kuvaev A. A. K vo-
prosu o chislenom modelirovanii istochnikov ra-
dioaktivnogo zagryazneniya gruntov i gruntovykh
vod pri obosnovanii vyvoda radiatsionno-opasnykh
ob"yektov iz ekspluatatsii [On the Issue of Numerical
Simulation of Sources of Soil and Groundwater Ra-
dioactive Contamination to Be Used in the Substan-
tiation of Decommissioning of Radiation-Hazardous
Objects]. *Voprosy radiatsionnoy bezopasnosti — Ra-
diation Safety Issues*, 2019, no. 4 (96), pp. 3–12.
19. Kapyrin I. V. Raschetnye kody dlya gidrogeo-
logicheskogo modelirovaniya v zadachakh otsenki
bezopasnosti OIAE [Computational Codes for the
Hydrogeological Modeling in the Safety Assess-
ment of Nuclear Facilities]. *Radioaktivnye otkhody —
Radioactive Waste*, 2022, no. 2 (19), pp. 105–118.
DOI: 10.25283/2587-9707-2022-2-105-118.
20. Serebryakov B. E. *Modelirovaniye rasprostraneni-
ya radioaktivnykh veshchestv v okruzhayushchey srede*
[Modeling the distribution of radioactive substances
in the environment]. Moscow, Burnazyan Federal
Medical Biophysical Center of the FMBA of Russia
Publ., 2022. 188 p.

Information about the authors

Anisimov Nikolay Alexandrovich, Chief Specialist of GIS Technologies and Mathematical Modeling Department, FSBI “Hydrospetzgeologiya” (4, Marshal Rybalko st., Moscow, 123060, Russia), e-mail: anisn@bk.ru, e-mail: anisn@msnr.ru.

Kuvaev Andrey Alekseevich, Doctor of geological and mineralogical sciences, Chief of GIS Technologies and Mathematical Modeling Department, FSBI “Hydrospetzgeologiya” (4, Marshal Rybalko st., Moscow, 123060, Russia), e-mail: andrey_kuvaev@inbox.ru, e-mail: kuvaev@msnr.ru.

Sizonenko Elena Vladimirovna, Leading Specialist of GIS Technologies and Mathematical Modeling Department, FSBI “Hydrospetzgeologiya” (4, Marshal Rybalko st., Moscow, 123060, Russia), e-mail: Butterfly16@list.ru, e-mail: sizonenko@msnr.ru.

Bibliographic description

Anisimov N. A., Kuvaev A. A., Sizonenko E. V. Numerical modeling of nuclide transport in structures and the near field of a near-surface radioactive waste disposal facility. *Radioactive Waste*, 2023, no. 4 (25), pp. 89–100. DOI: 10.25283/2587-9707-2023-4-89-100. (In Russian).